mathematics

MDPI

Article

Methodology for Transient Stability Assessment and Enhancement in Low-Inertia Power Systems Using Phasor Measurements: A Data-Driven Approach

Mihail Senyuk [1], Svetlana Beryozkina [2], Ismoil Odinaev [1], Inga Zicmane [3,*] and Murodbek Safaraliev [1]

[1] Department of Automated Electrical Systems, Ural Federal University, 620002 Yekaterinburg, Russia; mdseniuk@urfu.ru (M.S.); ismoil.odinaev@urfu.ru (I.O.); murodbek_03@mail.ru (M.S.)
[2] College of Engineering and Technology, American University of the Middle East, Egaila 15453, Kuwait; svetlana.berjozkina@aum.edu.kw
[3] Faculty of Electrical and Environmental Engineering, Riga Technical University, 12/1 Azenes Str., 1048 Riga, Latvia
* Correspondence: inga.zicmane@rtu.lv

Abstract

Modern energy systems are undergoing a profound transformation characterized by the active replacement of conventional fossil-fuel-based power plants with renewable energy sources. This transition aims to reduce the carbon emissions associated with electricity generation while enhancing the economic performance of electric power market players. However, alongside these benefits come several challenges, including reduced overall inertia within energy systems, heightened stochastic variability in grid operation regimes, and stricter demands on the rapid response capabilities and adaptability of emergency controls. This paper presents a novel methodology for selecting effective control laws for low-inertia energy systems, ensuring their dynamic stability during post-emergency operational conditions. The proposed approach integrates advanced techniques, including feature selection via decision tree algorithms, classification using Random Forest models, and result visualization through the Mean Shift clustering method applied to a two-dimensional representation derived from the t-distributed Stochastic Neighbor Embedding technique. A modified version of the IEEE39 benchmark model served as the testbed for numerical experiments, achieving a classification accuracy of 98.3%, accompanied by a control law synthesis delay of just 0.047 milliseconds. In conclusion, this work summarizes the key findings and outlines potential enhancements to refine the presented methodology further.

Keywords: power system; transient stability; emergency control; machine learning; clustering algorithm; low inertia; renewable energy sources

MSC: 68T01

check for updates

Academic Editor: Giancarlo Consolo

Received: 18 August 2025
Revised: 21 September 2025
Accepted: 3 October 2025
Published: 5 October 2025

Citation: Senyuk, M.; Beryozkina, S.; Odinaev, I.; Zicmane, I.; Safaraliev, M. Methodology for Transient Stability Assessment and Enhancement in Low-Inertia Power Systems Using Phasor Measurements: A Data-Driven Approach. *Mathematics* **2025**, *13*, 3192. https://doi.org/10.3390/math13193192

1. Introduction

Control of electric power system (EPS) modes falls into the category of optimization problems under uncertain conditions regarding the electrical regime and parameters of equivalent circuits for power equipment. For designing control laws governing normal and transient processes in traditional EPS, deterministic methods have traditionally been employed. These methods rely on solving systems of differential-algebraic equations that describe energy transformation and transmission in electric circuits [1]. Such deterministic approaches are practical in traditional EPS dominated by fossil fuel-based generation, where sufficient inertia ensures stable operation. However, modern transformations in EPS introduce profound changes affecting transient process dynamics, generation capacity structures, and control methodologies [2]. Specifically, the increasing penetration of renewable energy sources (RES), the widespread adoption of power-electronics-based control devices, and the deployment of Flexible Alternating Current Transmission Systems (FACTS) concurrently with the phasing out of fossil fuel power plants result in diminished inertia and amplified oscillations, as well as faster transients [3]. Under these evolving operational conditions, traditional deterministic control strategies cannot meet heightened demands for rapidity and adaptability in selecting control actions (CAs).

Deterministic algorithms for synthesizing emergency control laws in EPS require substantial preprocessing computations using predefined input data. Consequently, the determination of optimal CAs incurs delays tied to the cycle of updating information. In low-inertia environments typical of future EPS, such delays risk rendering controls either inadequate or overly aggressive, given the dramatic shifts in electrical regimes occurring between updates of the emergency control law. Beyond changes in generation mixes and control paradigms, another defining trait of next-generation EPS is their growing reliance on digitization and massive data collection. This trend facilitates the emergence of intelligent monitoring and control systems that can leverage advanced analytics [4]. Therefore, enhancing the adaptability and responsiveness of emergency control systems becomes crucial for ensuring the timely and appropriate execution of control actions amidst reduced inertia and accelerated transient phenomena.

The reduction in the inertial component in modern EPS has the most significant impact on ensuring transient stability (TS), which becomes more challenging due to the increased speed of transient processes, despite the active implementation of control systems that provide synthetic inertia [5]. To meet the requirements of modern EPS in terms of adaptability and responsiveness, machine learning (ML) algorithms can be effectively applied. This class of supervised learning algorithms enables the identification of complex correlations based on training data, thereby determining the correspondence between electrical regime parameters and CA [6]. When using unsupervised learning, control laws are synthesized based on the results of the interaction between the control agent and the environment being studied. The agent's actions are aimed at maximizing the reward function, which determines the optimality of the CA [7]. From the perspective of ML algorithms, the task of emergency control of EPS regimes is a classification problem with multiple classes that define control actions. The parameters of the electrical regime describe the attributes or features of the classification [8], which form a variable space in which the classification procedure is performed.

When using unsupervised ML algorithms, the diagram shown in Figure 1 will change in terms of algorithm training, while the operational stage will remain unchanged. Unsupervised ML algorithms determine decision rules during interaction with the environment under study, so they do not require preparing a data sample. The source of data for training the ML algorithm is a combination of physical and synthetic data. The source of physical data can be EPS emergency control systems, which are based on deterministic algorithms [9]. The combination of synthetic and physical data ensures the representativeness and sufficiency of the data sample, which allows it to be used for training ML algorithms. Based on the generated data sample, a CA is selected to ensure the considered parameter of the post-emergency mode [10]. Next, the generated data sample is processed to eliminate noise, outliers, balance classes, and select informative features. The collected data is used for pruning, testing, and validating the considered ML algorithms [11].

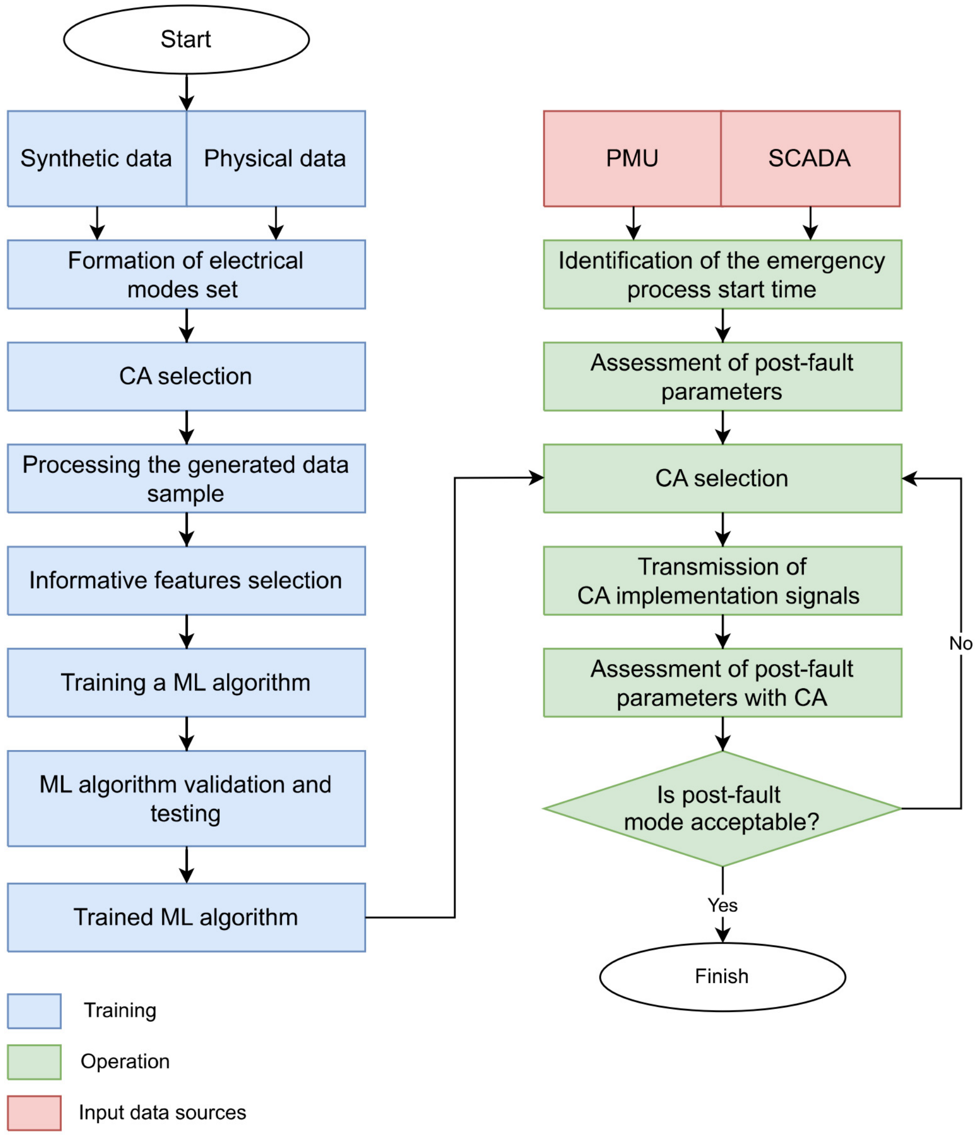

Figure 1. General structure of the emergency control complex for EPS operating modes based on ML algorithms.

At the operational stage, the sources of initial data are measurements obtained from phasor measurement units (PMU) [12] and supervisory control and data acquisition (SCADA) systems. Based on the acquired measurements, procedures are performed to identify the type and location of a short circuit (SC) [13,14] or other disturbance that causes dangerous measurements of the electrical mode from the perspective of TS. Using pre-emergency parameters of the electrical mode and information on the type of disturbance, an assessment of the TS of the post-emergency mode is performed. When identifying the loss of TS, the selection of optimal CA is performed, followed by its implementation. After the implementation of CA, a repeated assessment of TS is performed; in case of identifying the insufficiency of CA, they are re-selected and implemented [15].

The emergency control organization scheme shown in Figure 1 can be applied both in traditional and in EPS with reduced inertia. In the latter case, it is necessary to develop accelerated algorithms for synchrophasor evaluation, disturbance type and location identification, TS evaluation, and CA selection. Most of these challenges can be effectively addressed by employing ML algorithms. The objective of this study is to enhance the methodology outlined in [16] from the perspective of CA selection for EPS operating modes with TS loss.

2. Current State of the Problem

The task of TS analysis and CA selection for maintaining stability of the post-accident scheme is characterized by high nonlinearity [17]. Typically, the solution to such problems relies on computationally complex deterministic methods involving the numerical analysis of systems of differential-algebraic equations that describe the dynamic model of the protected EPS. Despite this complexity, modern EPS emergency control systems are subject to high requirements for speed, adaptability, and accuracy of mode parameters. ML algorithms stand out as one of the most promising classes of methods for EPS TS assessment and CA selection, meeting these requirements. These algorithms are capable of uncovering hidden and implicit correlations in data, providing a solution to the problem of emergency control of EPS operating modes with minimal delay compared to deterministic methods [18]. To date, researchers have proposed the following ML algorithms to accelerate the solution of the TS analysis and CA selection problem:

- eXtreme Gradient Boosting (XGBoost) [19];
- Deep learning (DL) [20];
- Support vector machine (SVM) [21];
- Autoencoder [22];
- Graph neural network (GNN) [23];
- Deep belief network (DBN) [24];
- Deep reinforcement learning (DRL) [25];
- Lyapunov neural network (LNN) [26];
- Stacking of multilayer perceptrons [27];
- Least square support vector machine (LS-SVM) [28].

In the work [19], the extreme gradient boosting algorithm is employed to estimate the EPS TS. Let us denote this algorithm as A1. The choice of A1 is motivated by its high speed in the training and testing process, the absence of the need for a data preprocessing stage, and the presence of a built-in regularizer. The latter is designed to prevent the algorithm from overfitting by introducing a limitation on the obtained parameters. One of the stages of constructing A1 involves the selection of dominant input features from the dataset. For this purpose, the work utilizes a procedure for calculating the mutual correlation of features, with a threshold value of 0.98. The method was tested using the IEEE 39 power system model. A detailed description of the division of the dataset into training and test samples is not provided in the work. The authors propose the operating mode parameters of each synchronous generator (SG) as input features of A1 for solving the EPS TS analysis problem. The work compares A1 with the following algorithms: random forest (RF), decision tree (DT), SVM, and artificial neural network (ANN). The accuracy of A1 in classifying the loss or preservation of EPS TS in post-accident mode was 97.82% with a time delay of 11 ms. Thus, A1 proved to be the most accurate compared to the other listed algorithms. The positive aspect of the algorithm is its robustness to outliers in the initial data and the absence of resource-intensive and complex mathematical functions. The negative aspect of the algorithm is the effect of overtraining.

To analyze the preservation of EPS TS, the paper [20] proposes the use of a deep learning algorithm. Let us denote this algorithm as A2. The electrical mode parameters transmitted by PMU are used as input features for forming the dataset. The EPS TS is estimated based on the disturbance severity index calculation method. This method takes into account changes in the module, phase, and frequency in the EPS nodes. Transient processes were simulated based on the IEEE39 and IEEE118 EPS power system models. As a result, synthetic data were generated in 3528 and 2476 transient processes for the IEEE39 and IEEE118 models, respectively. When noise was imposed on the generated data in the range from 40 to 60 dB, the classification accuracy on the considered data samples varied from 99.12% to 99.64%. The positive side of A2 includes its high adaptability. Increasing the number of hidden layers in the presence of a large volume of training data can significantly enhance the generalization ability of the algorithm. The main disadvantage of A2 is the computational load due to the use of complex mathematical functions in neurons.

In [21], the EPS TS is estimated based on the SVM algorithm, which uses the Mahalanobis distance. We will further denote it as A3. The A3 algorithm enables the analysis of the DS for each SG. The training dataset used consisted of records of 1680 SG operating modes, each with a capacity of 300 MW. The testing results showed that the accuracy of A3 is 96.79%. The positive side of A3 is its low computational load. However, the efficiency of the algorithm is inversely proportional to the growth of the training data volume.

In [22], it is proposed to estimate EPS TS using an autoencoder. Let us denote this algorithm as A4. The input features for A4 are the data obtained from synchronized vector measurements. The training dataset was obtained based on numerical experiments performed for the IEEE50 model. In this model, three-phase SC's with durations of 0.1, 0.15, 0.2, and 0.3 s were modeled as disturbances in different EPS nodes. As a result, a dataset of 28,436 transient processes was formed, 70% of which related to disturbances with preservation of the control system, and the remaining 30% to disturbances with loss of TS. Testing of A4 is performed based on a numerical experiment, and its comparison with the following algorithms is carried out: support vector method, decision tree, K-nearest neighbors (KNN), RF, ANN, naive Bayes classifier (NBC), nearest centroid classifier (NCC), and XGBoost. As a result, the authors of [22] found that the accuracy of A4 is 97.23%, and the delay in classifying one transient process is 62 ms. Thus, A4, in comparison with the considered algorithms, proves to be dominant in accuracy, but in terms of performance, it is inferior to the algorithms of ANN, DT, and XGBoost. The positive aspects of A4 include its robustness to noise in the original data. The disadvantage of the algorithm is the need to use mathematical functions for the trained model.

In [23], the estimation of EPS TS is performed based on the GNN algorithm. Let us denote it as A5. The foundation of this network's operation for TS estimation is as follows: the stability of a node is determined by a combination of its internal characteristics and the characteristics of the external electrical network. TS is the result of the interaction of all generator nodes. Testing of A5 was carried out based on the mathematical models of the IEEE39 and IEEE300 EPS. For the first model, the algorithm's classification accuracy was 98.50%, and for the second model, it was 98.48%. As future work, the possibility of evaluating the dynamic stability of individual nodes is considered, which is a development of Dimo's theory of nodal equivalents [29]. The algorithm's advantage lies in its interpretability, which stems from data processing based on the physical principles of EPS. The primary disadvantage is the computational load resulting from the use of multiple models for step-by-step data processing.

In the study [24], the use of the DBN algorithm is proposed for selecting the CA to ensure EPS TS in post-accident operation mode. Let us designate it as A6. As the objective function of emergency control, the equation is proposed:

$$minC = min \sum_{i \in S_G} (r_i^{up} \Delta P_i^{up} + r_i^{down} \Delta P_i^{down}), \tag{1}$$

where C is the total cost of emergency control, i is the number of SGs connected to the control unit, r is the cost of loading or unloading the SG, and ΔP is the change in SG capacity by increasing or decreasing.

Algorithm A6 consists of two DBNs. The first is designed to assess TS, while the second is intended for selecting CA. For training the networks, a series of transient processes was synthesized based on the mathematical model of the South Carolina power system, which has 500 nodes. The validation results showed that the accuracy of A6 in classification was 99.15%, and its time delay for one transient process was 0.01 s. The advantage of A6 lies in its flexibility due to the ability to increase the number of neurons and layers. The drawback of the algorithm is its relatively high computational complexity.

In [25], it is proposed to use a DRL for selecting CA to ensure TS in the post-fault operation mode of the EPS. Let us denote this algorithm as A7. The structure of the emergency control block consists of two modules: an agent and an environment. The agent is the emergency control system capable of generating CA, while the environment is the EPS. The algorithm was tested based on the mathematical models of the IEEE39 and NPCC140 EPS. A comparison of the proposed algorithm for classifying CA with the particle swarm optimization method was conducted. As a direction for future research, the paper suggests testing the algorithm on real EPS data. The positive aspect of A7 is its flexibility, which enables the solution of problems involving complex dynamic systems. The negative aspect of the algorithm is its long training time and relatively high computational complexity.

In [26], the selection of CA for ensuring EPS TS is performed based on an LNN. Let us denote this algorithm as A8. The algorithm was tested on the mathematical models of the IEEE9, IEEE39, and IEEE118 power systems. In the computational experiments, A8 is compared with a linear-quadratic regulator. The advantage of algorithm A8 is its flexibility. Its disadvantage is the high computational load.

In [27], a stacking was formed from a set of separately taken multilayer perceptrons. Let us denote this algorithm as A9. The input features of the algorithm for selecting CA to maintain TS in the post-fault operation mode of the EPS are the active powers of SGs, the modules, and the phases of voltages in the EPS nodes. When a loss of dynamic stability is detected, the selection of CA is performed in the EPS regime optimization block with dynamic constraints. To form the dataset, a series of 5000 electromechanical transient processes was generated based on the mathematical model of the IEEE39. Approximately 56% of these data relate to transient processes without CA, and the remaining part relates to transient processes with CA. In [27], A9 is compared with the following algorithms: RF, SVM, convolutional neural network (CNN), autoencoder, and DBN. As a result, it was shown that the proposed method was the most effective with an accuracy of 98.55%. The positive aspect of the algorithm is its flexibility due to the number of feedforward neural networks and layers in them. The drawback of the algorithm is its computational complexity.

In [28], the selection of CA for ensuring EPS TS is performed based on the LS-SVM method. Let us denote this algorithm as A10. The input features are the amplitude and phase of voltages measured by synchronized vector measurement devices. A numerical experiment is carried out based on the IEEE39 mathematical model. The positive aspect of the algorithm is its fast training. Its negative side is its sensitivity to outliers in the data.

For clarity, the characteristics of the above-described algorithms A1–A10 are compared in Table 1. In the columns for CA and TS, the symbol «+» indicates the algorithm's ability to select CA and assess the EPS TS.

The issue of developing a methodology for selecting the control unit and assessing the control system of the EPS is described in detail in the considered works. In the considered works, algorithms based on neural networks and deep learning are mainly proposed to solve the problem. This allows for an acceptable level of accuracy and adaptability of the solution to the problem of emergency control of the EPS operating modes. Moreover, the use of multilayer and nested ML algorithms allows for the identification of hidden and implicit patterns in the data sample. The testing of the considered algorithms A1–A10 is carried out using synthetic data generated as a result of a series of numerical experiments based on the EPS models IEEE9, IEEE39, IEEE118, NPCC140, and IEEE300. The accuracy of these classification algorithms on test data varies in the range from 97.23% to 99.64%. Additionally, several of the considered works assess the robustness of the algorithm to noise in the original data.

Table 1. Analysis of methods for assessing EPS TS and selecting CA.

Ref.	Method	CA	TS	Advantages and Drawbacks
[19]	A1		✓	(+) robustness to outliers in the data and the absence of complex mathematical functions (−) overfitting effect
[20]	A2		✓	(+) high adaptability, possibility to increase generalization ability (−) computational load due to complex mathematical functions in neurons
[21]	A3		✓	(+) low computational load (−) efficiency decreases with increasing data volume
[22]	A4		✓	(+) robustness to noise in the initial data (−) need to apply mathematical functions after training
[23]	A5		✓	(+) interpretability due to the algorithm's operation based on the physical principles of EPS (−) computational load depends on the set of models used
[24]	A6	✓	✓	(+) flexibility due to the increase in the number of neurons and layers (−) preservation of mathematical functions after training
[25]	A7	✓	✓	(+) high flexibility due to the number of layers (−) long training and relatively computational complexity
[26]	A8	✓	✓	(+) high flexibility due to the number of layers (−) comparatively high computational load
[27]	A9	✓	✓	(+) flexibility due to the number of feedforward neural networks and layers (−) computational complexity
[28]	A10	✓	✓	(+) fast learning (−) sensitivity to outliers in data

Among the disadvantages of the reviewed studies, the following can be highlighted: the lack of consideration for changes in the topology of the EPS in the training and test datasets, insufficient development of the task of estimating the time delay in CA selection, and the use of a non-verified algorithm for selecting CA as a reference for generating the dataset. To compensate for the described shortcomings of algorithms A1-A10 for selecting CA and ensuring TS in post-fault operation modes of the EPS, a new methodology is proposed in this work. This methodology is based on the application of an algorithm for selecting CA that has been adopted for industrial use. When generating the dataset, the schematic and operational diversity is taken into account by changing the topology of the test EPS [30]. The classification time delays are determined.

3. Methodology for Selecting CA to Ensure EPS TS Based on ML Algorithms

EPS TS is one of the key types of stability, the requirements for which have changed significantly due to the reduction in constant inertia. When EP occurs with the disconnection of the power transmission line, SG or SC, an accelerating moment acts on the SG rotors, leading to an increase in the angular velocity of rotation of the rotor and a loss of stability. A sufficient condition for maintaining EPS TS is the fulfillment of the following equality in the space of the SG rotor moment and the load angle:

$$J \cdot \frac{(w_0 + \Delta w)^2 - w_0^2}{2} = \int_{\delta_s}^{\delta_f} (M_T - M_{SG}) d\delta - \Delta W_d, \tag{2}$$

where J is the moment of inertia of the SG rotor and turbine, M_T is the accelerating torque created by the turbine, M_{SG} is the braking torque created by the SG magnetic field, w_0 is the angular velocity of the SG rotor before the occurrence of EP, Δw is the change in the angular velocity of the SG rotor by the end time of SC, δs is the load angle of the SG before the occurrence of EP, δ_f is the load angle of the SG by the end time of SC, ΔW_d is the energy spent on damping the oscillations of the SG rotor and turbine.

Equation (2) describes the law of conservation of energy in EPS. When EPS EP occurs, an imbalance of active power occurs, leading to an excess of the accelerating torque with an increase in the load angles SG's. When the load angle along the power transmission lines exceeds the value of 360 degrees, an out-of-step cutset is formed with the division of EPS into several parts. In the general case, the division of EPS fragments occurs with negative or positive imbalances of active power depending on the pre-emergency directions of active power flows along the power transmission lines. An example of the division of EPS into fragments is shown in Figure 2.

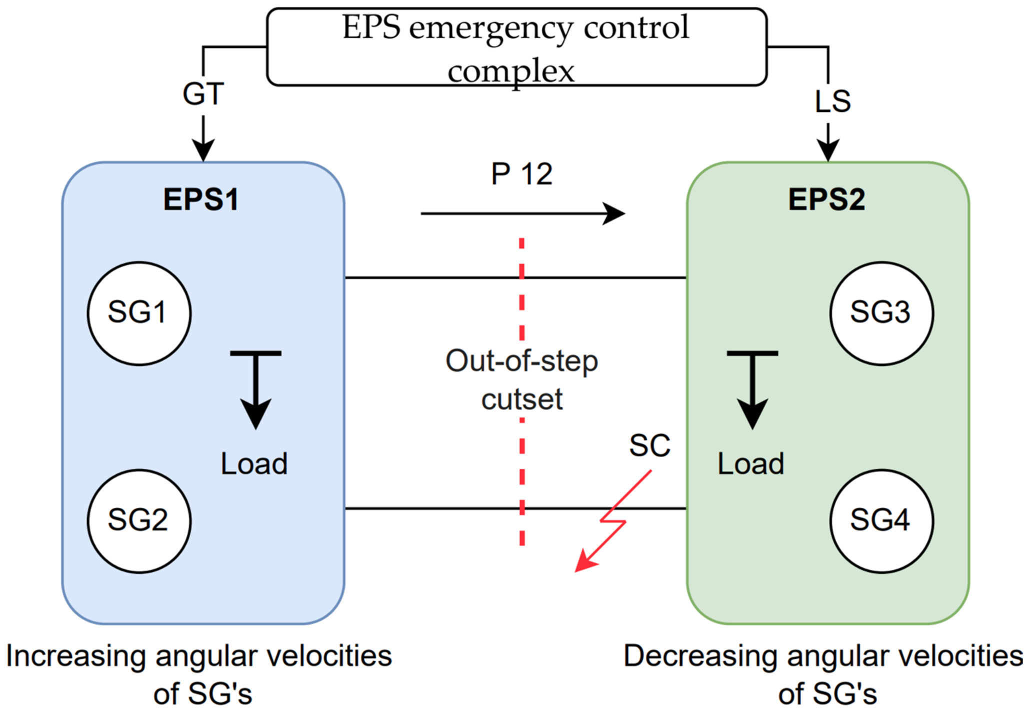

Figure 2. Illustration of the CA selection principle.

When SC occurs on one of the two parallel transmission lines connecting EPS1 and EPS2, an asynchronous running section occurs, limiting the transmission of active power, shown in Figure 2 by the designation "P 12". Thus, in EPS1, an excess of active power occurs, leading to an increase in the angular velocities of SGs. In EPS2, a deficit of active power occurs, accompanied by a decrease in the angular velocities of SGs. To maintain EPS TS, GT-type CA is used in EPS1, and LS-type CA is used in EPS2. This method of organizing EPS control enables maintaining TS in post-emergency mode.

To implement the EPS emergency control complex, information about EPS operation parameter measurements, a mathematical model of the protected EPS, and a list of possible CAs and EP parameters are utilized. Figure 3 shows an example of input and output information for the EPS emergency control complex. Based on the information received from SCADA and PMU, the EP parameters are identified, including the type, location, and parameters of the EP. Using the mathematical model of the protected EPS, the state estimating procedure is performed, and the optimal CAs are selected to ensure EPS TS.

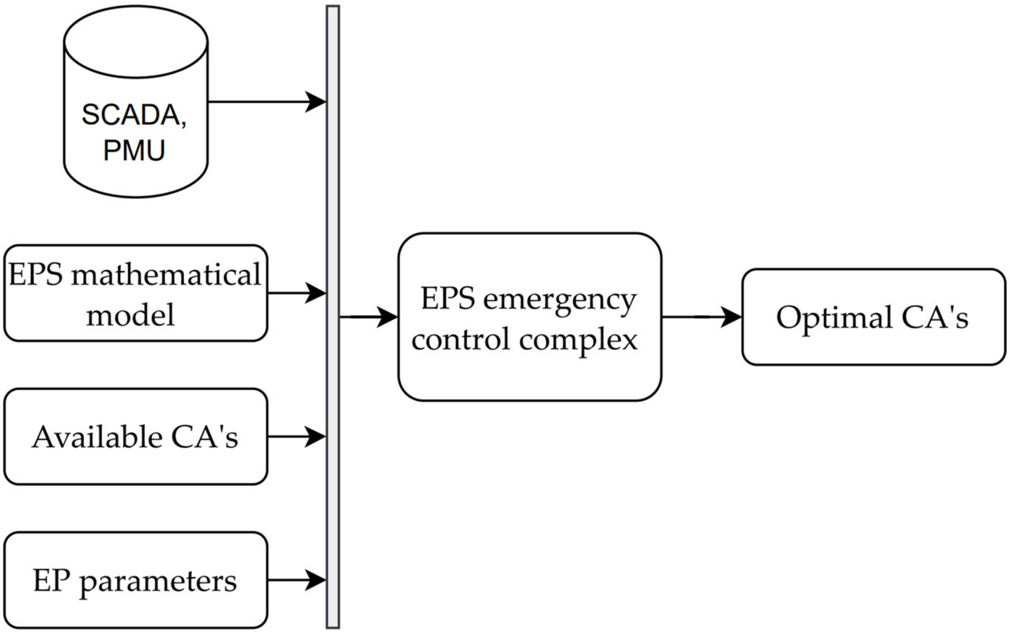

Figure 3. Input and output data for the EPS of the emergency control complex.

The proposed methodology for selecting CA to ensure TS in the post-fault operation mode of the EPS represents a pipeline structure [31], organizing the end-to-end process of synthesis, data preparation, training, and testing of ML algorithms, as well as the analysis of the classification quality of the CA type. Figure 4 shows the block diagram of the proposed methodology.

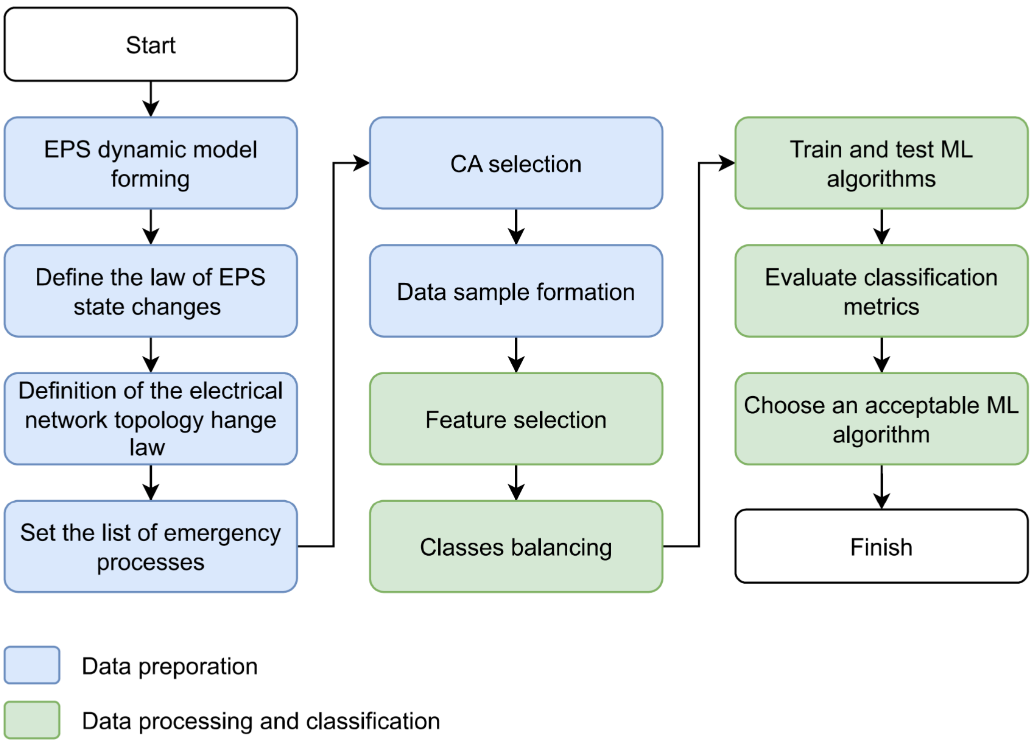

Figure 4. The proposed method for CA selection to ensure EPS TS based on ML algorithms.

From the perspective of machine learning theory, the task of choosing a CA falls under multiclass classification, where electrical mode parameters serve as features and types of CA represent classes. The input data for solving this classification problem consists of samples describing changes in features and classes depending on the scheme-regime situation, which is influenced by the topological configuration of the electrical network and power flow distribution. Data samples can be obtained either through real-time deterministic anti-emergency management systems or via mathematical modeling. Both approaches have their advantages and disadvantages. Real-world data from actual deterministic anti-emergency management systems describe genuine transient processes considering the actual state of the EPS, but face limitations due to the inability to consider atypical regimes and calculate unexamined emergency processes (EPs) [32]. On the other hand, synthetic data do not reflect processes in real-life EPSs; however, they allow arbitrary schematic-regime scenarios and practically any EPs during mathematical simulations.

The first stage of the proposed methodology involves specifying the initial data required for varying the analyzed schematic-regime situations. In the study, numerical simulation results of electromechanical transient processes in the mathematical model of the EPS were utilized as the source of data. To achieve diversity in schematic-regime configurations, variations are introduced into the states of transmission lines, load values at EPS nodes, and generation levels of SGs. Additionally, loads at EPS nodes vary according to predefined laws with random components added that follow normal distributions. Furthermore, the input information includes a list of considered EP, which in this research specify the type of SC, its location, and duration [33].

After constructing the dynamic model of the EPS and compiling the list of input data, the simulation of electromechanical transient processes is carried out, followed by the evaluation of loss of TS and selection of CA using a verified algorithm [1]. Generally speaking, any algorithm accepted as a reference may be employed for CA selection. The resulting choice is presented in matrix form, where rows correspond to modes described by unique schematic-regime situations, columns include the type of CA, features characterizing the parameters of the electrical mode, and a description of the relevant EP. The type of CA implies the determination of the place and volume of disconnection of SG or load in the nodes of the EPS.

The learning speed of the ML algorithm, like any optimization algorithm, significantly depends on the dimensionality of the solved problem, i.e., the number of features considered during solution search. When creating a dataset for selecting CA to maintain TS in post-fault operation mode of the EPS, there exist several features exerting minimal influence on the classification result. Such features could include active power flows along transmission lines feeding dead-end substations, voltages in remote nodes of the EPS away from the fault point, etc. Expert identification of these features is labor-intensive and often non-trivial, given the changing schematic-regime situation. Selection of significant features is achieved by calculating feature importance for DT algorithms [34], which rely on partitioning the input sample set at each node based on logical rules over selected features aimed at reducing entropy in sub-samples. Features are ranked by significance depending on how frequently they appear in logical rules as output from the decision tree algorithm; a vector of features and corresponding significance values expressed by the Gini coefficient [35] is generated. Experts can determine a threshold value for significance, eliminating a feature from further use in training and testing classification algorithms. In this study, the threshold significance value was chosen equal to 0.03, meaning that if the Gini coefficient is less than 0.03, then such a feature is removed from the dataset. This threshold significance value might change depending on the specific EPS model and the range of CA and EP being considered. Automatic selection of the threshold significance value has not been addressed in this study and remains a subject for future research.

One of the requirements imposed on a dataset intended for training ML algorithms is balance, i.e., representation of each class in equal proportions within the dataset. If the dataset is imbalanced, the ML algorithm may train predominantly on the most frequent class, thereby ignoring the least represented ones, rendering it ineffective when applied to new data. Several methods can be employed to ensure balanced sampling [36], including class weighting, oversampling, and undersampling. Class weighting assigns weights to each class. The weight factor's value is determined based on the proportion of the class in the dataset. However, this introduces additional complexity because determining the appropriate weight vector adds another degree of freedom to the classification process, making overall data preparation more uncertain. Oversampling and undersampling involve adjusting the quantity of data in the dataset by removing or duplicating specific modes. Undersampling is applicable only when sufficient data exists, including an adequate representation of minority classes. Oversampling does not provide a reliable way to capture patterns characteristic of minority classes. Due to the limitations associated with class weighting, oversampling, and undersampling, the most commonly adopted techniques are those involving the synthesis of artificial data. These methods generate new data points based on existing examples of the minority class, preserving underlying patterns. Two widely recognized methods for generating synthetic data are the synthetic minority oversampling technique (SMOTE) and adaptive synthetic sampling. Both techniques synthesize new modes by interpolating between neighboring instances identified through Euclidean distance calculations. Adaptive synthetic sampling additionally considers the difficulty of classifying the type of CA, leading to slower performance compared to SMOTE. Therefore, in this study, we employ the SMOTE method to balance classes in the dataset.

The processed dataset, considering the selection of significant features and class balancing, is utilized for training and testing ML algorithms. The division of the dataset into training and test sets follows an 80/20 ratio. Training of the ML algorithms entails hyperparameter tuning through grid search [37], whose nodes are defined by expert judgment. For this investigation, the following ML algorithms have been selected: Linear Regression (LR), k-Nearest Neighbors (KNN), Random Forest (RF), eXtreme Gradient Boosting (XGBoost), AdaBoost, CatBoost, Light Gradient Boosting Machine (LightGBM), Support Vector Machines (SVM), and Restricted Boltzmann Machines (RBM) [38]. The choice of ML algorithms reflects a compromise between computational complexity, adaptability, and the ability to uncover fuzzy and hidden correlations within the data.

Standard metrics [39] were used to assess the quality of the classification. The data quality assessment was based on the Mean shift clustering [40] algorithm with the calculation of the following clustering quality metrics: Silhouette coefficient, Davies-Bouldin index, Calinski-Harabasz index, Adjusted Rand index, Homogeneity score, V-measure score [41]. An additional metric reflecting the quality of the trained ML algorithm's performance is the classification delay incurred by the ML algorithm when identifying the type of CA for one EP.

The scientific novelty of the study lies in developing a methodology for selecting CA to ensure TS EPS, providing the required levels of speed and adaptability dictated by modern EPS with a significant share of RES.

4. Case Study

Validation of the proposed control action selection methodology for ensuring dynamic stability was carried out using the mathematical model of the power system IEEE39 [42]. This model consists of 10 SGs, simulated to account for turbine models, automatic voltage regulators, and system stabilizers, as well as 39 nodes and 46 transmission lines. The graphical representation of the modified IEEE39 model is shown in Figure 5. In this model, all SGs are connected to the electrical grid through block step-up transformers. SG1 simulates a connection to an external power system; hence, it is directly connected to node 39, while the remaining SGs represent equivalent power plants. For modeling electromechanical transient processes, selecting CAs, processing data samples, training, and testing machine learning algorithms, the Python 3 development environment was utilized, employing parallel computations on graphics processors. For modeling wind generators (WG), the model and graphs of generated active power from [43] were used. The procedure for forming a data sample is described in detail in studies [6,43], and a similar procedure is used in this study.

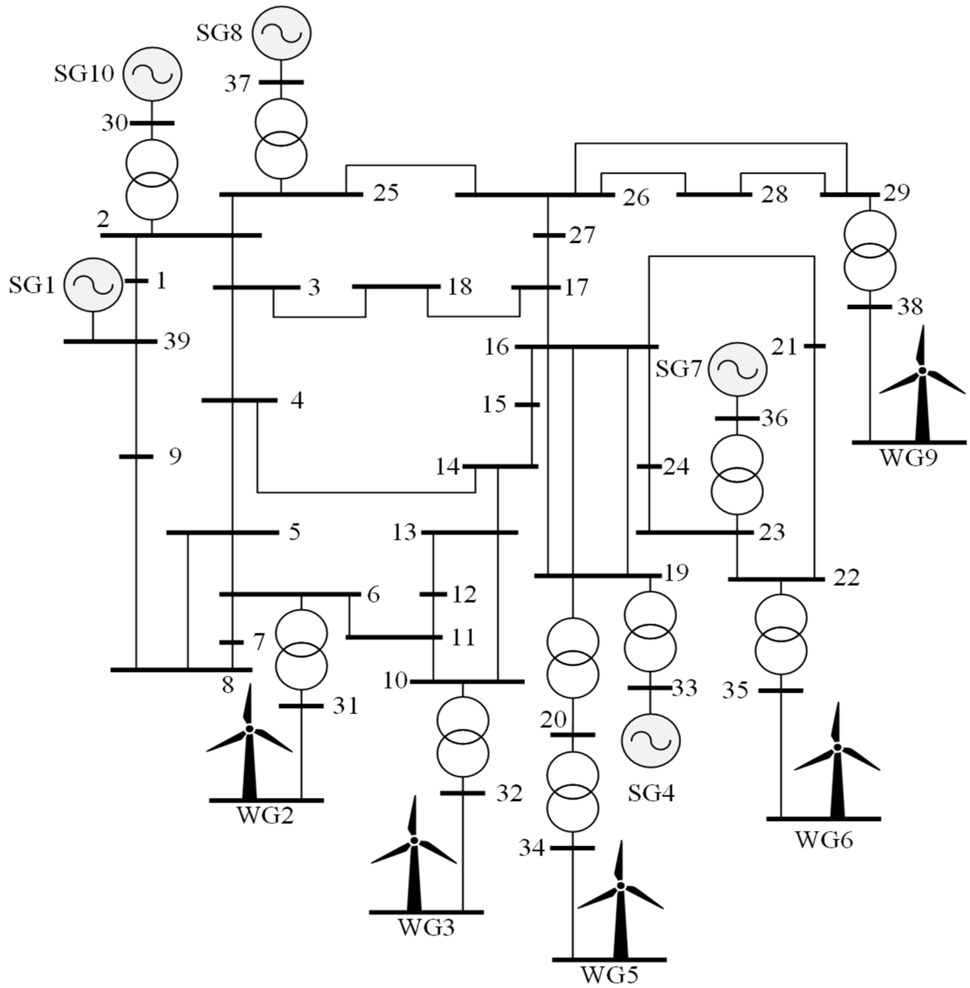

Figure 5. Modified IEEE39 mathematical model (WGs have been added to nodes 31, 32, 34, 35, and 38).

Table 2 shows the values of base loads in the IEEE39 model nodes with the CA presence flag of the load scheduling (LS) type. Table 3 shows the following SG parameters: P_{nom} is the SG nominal active power, T_j is the mechanical inertia constant of the unit, x_d is the synchronous inductive resistance of the armature winding along the longitudinal axis, x_d' is the transient inductive resistance of the armature winding along the longitudinal axis, x_d'' is the subtransient inductive resistance of the armature winding along the longitudinal axis, GT is the flag of the possibility of implementing the generator tripping type AC on SG. In this study, only two types of CA are used to ensure the TA: GT and LS. The use of the steam turbine fast valving [44] unloading type CA for centralized emergency control is a direction for future research.

Table 2. Load values in the nodes of the IEEE39 test mathematical model.

Node	Load, MVA	LS	Node	Load, MVA	LS
1	97.6 + j44.2		21	274.0 + j115.0	
2	322.0 + j2.4		23	247.5 + j84.6	
4	500.0 + 184.0	+	24	308.6 + j92.2	
7	233.8 + j84.0	+	25	224.0 + j47.2	
8	522.0 + j176.0	+	26	139.0 + j17.0	+
12	8.5 + j88.0	+	27	281.0 + j75.5	+
15	320.0 + j153.0		28	206.0 + j27.6	+
16	329.0 + j32.3		29	283.5 + j26.9	+
18	158.0 + j30.0	+	31	9.2 + j4.6	+
20	680.0 + j103.0	+	39	1104.0 + j250.0	

Table 3. SG and WG parameters.

SG/WG	P_{nom}, MB_T	T_j, s	x_d, p.u.	x_d', p.u.	x_d'', p.u.	GT
1	1040	4.20	0.82	0.25	0.008	
2	646	–	–	–	–	+
3	725	–	–	–	–	
4	652	2.86	2.16	0.36	0.008	+
5	508	–	–	–	–	+
6	687	–	–	–	–	
7	580	2.64	2.43	0.41	0.008	
8	564	1.43	2.39	0.47	0.008	+
9	865	–	–	–	–	+
10	1100	5.00	0.18	0.05	0.009	

Table 4 describes the classes used. The «GT» column provides the SG numbers where the GT-type AC is used within one class, and the «LH» column provides the node numbers where 100% load scheduling [45] is performed when implementing the CA. In the numerical example, eight distinct classes of CAs are implemented. These classes are dynamically chosen according to both the network topology and specific operational conditions of the electrical system. A deterministic algorithm, initially introduced in reference [1], has been appropriately adapted and enhanced to guarantee TS within the given framework.

Table 4. Description of classes.

Class Number	GT	LS
0	WG2	Node 8
1	SG4	Node 12
2	WG5	Node 15
3	SG8	Node 16
4	WG9	Node 18
5	WG2 + WG5	Node 8
6	SG8 + WG9	Node 12
7	WG2 + SG8	Node 15

To form the data sample, the procedure of changing the parameters of the electrical mode with subsequent calculation of EP and selection of CA, presented in Figure 2, was used. The following parameters of the electrical mode and calculated EP were used as features of the data sample: active power SG or WG, reactive power SG or WG, modules and phases of voltage in the nodes of the EPS test model, flows of active and reactive powers along the elements of the electrical network, active and reactive conductivity of short-circuit shunts, short-circuit duration, operational state of the elements of the electrical network [46]. The classes in the formed data sample are a complex value that combines the node number, type, and volume of CA. Figure 6 shows an example of measuring the following features in the generated data sample: active power flow along branch 3–17, reactive power flow along branch 4–14, and active power flow along line 15–14.

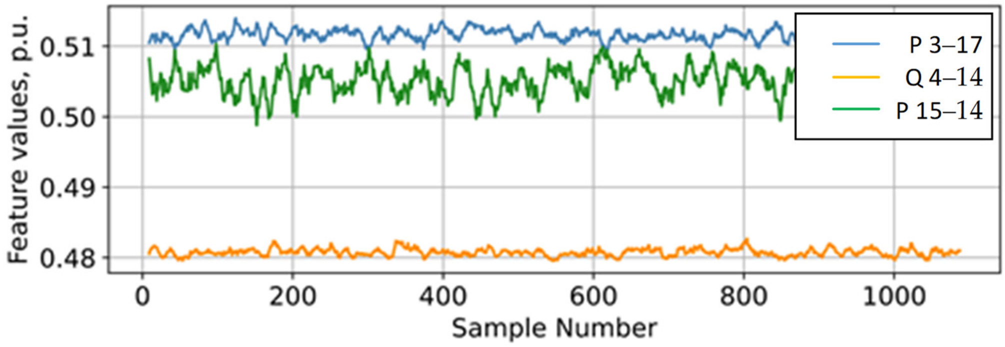

Figure 6. Changes in three features are presented in the data sample.

Figure 4 shows the changes in the parameters of the electrical mode of the EPS mathematical model, with values expressed in relative units to maintain clarity in the figure. The values of the parameters of the electrical mode reflect fluctuations caused by changes in loads, states of the elements of the electrical network, and the values of active power WGs.

To reduce the dimensionality of the CA volume classification problem being solved, a procedure for selecting the most significant features based on the DT algorithm [47] is used. The Gini coefficient is used as a feature significance metric. Figure 7 shows the correlation matrix of the selected informative features with the most tremendous significance for the CA volume classification problem.

To balance the classes in the generated sample, the SMOTE algorithm was used [48]. This method involves creating new instances in the data sample that correspond to classes with the smallest quantitative representation. The use of an unbalanced sample is reflected in the undertraining of the ML algorithms and the ignoring of minor classes. The most significant number of modes corresponds to class 6, the smallest to class 5. After applying the synthetic minority resampling method, the distribution of classes in the sample is uniform, while the number of modes in the data sample increased by 50%.

A necessary condition for applying the classification algorithm is the presence of data clustering, which makes it possible to construct a dividing surface. The most visual method of data cluster analysis is the analysis of the results of data dimensionality reduction algorithms: the principal component analysis (PCA), t-distributed Stochastic Neighbor Embedding (t-SNE) [49], multidimensional scaling, isometric mapping, etc. Figure 8 shows the results of clustering the generated data sample using the Mean shift [50] algorithm applied to the two-dimensional space of the first two t-SNE components. Since the t-SNE algorithm does not provide a physical interpretation of the coordinate axes, the axes in Figure 6 do not have physical dimensions. As a result of applying the Mean shift algorithm in the space of the first two t-SNE components, 8 clusters were identified, for describing the clustering quality of which the standard metrics given in Table 5 were used [51].

The matrix of correlations of informative features, given in Figure 5, shows the values of mutual correlations of the parameters of the electric mode taken into account during training and testing of ML algorithms. Each cell of the matrix shows the values of mutual correlation with the appropriate color highlighting. The symmetrical correlation matrix allows us to show only its lower part for the sake of clarity, since the upper part is completely symmetrical. The values of mutual correlations of the features taken into account during training and testing of ML algorithms are in the range from 0.05 to 0.96.

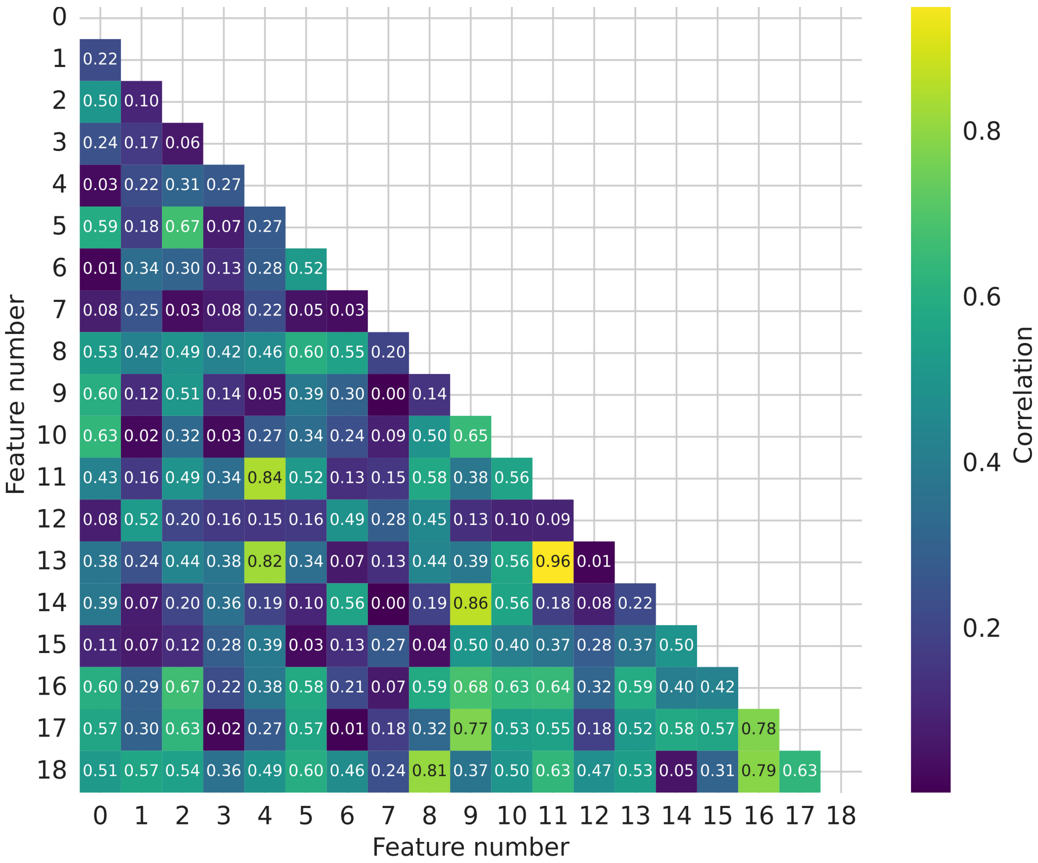

Figure 7. Feature correlation matrix.

Table 5. Classification quality metrics.

Metrics	Value
Silhouette coefficient	0.4440
Davies-Bouldin index	0.7483
Calinski-Harabasz index	1187.9363
Adjusted Rand index	0.5644
Homogeneity score	0.5213
V-measure score	0.5245

Figure 6 shows the graphical results of the cluster analysis of the data sample to which the t-SNE data dimensionality reduction algorithm was applied. The numbers of clusters identified by the Mean Shift algorithm are shown in color. The use of this data clustering algorithm made it possible to identify 8 clusters in the original data, corresponding to the number of CA classes under consideration, the description of which is given in Table 4.

The values of the silhouette coefficient and Davies-Bouldin index indicate a sufficient, but imperfect, quality of clustering. Excellent indicators were obtained for the Calinski-Harabasz index, allowing us to interpret the data sample as having a clear, structured separation of clusters. Despite the reduced values of the adjusted Rand index and homogeneity score, the data sample under consideration has sufficient properties for applying classification algorithms based on ML algorithms.

Table 6 shows the results of preliminary processing of the data sample.

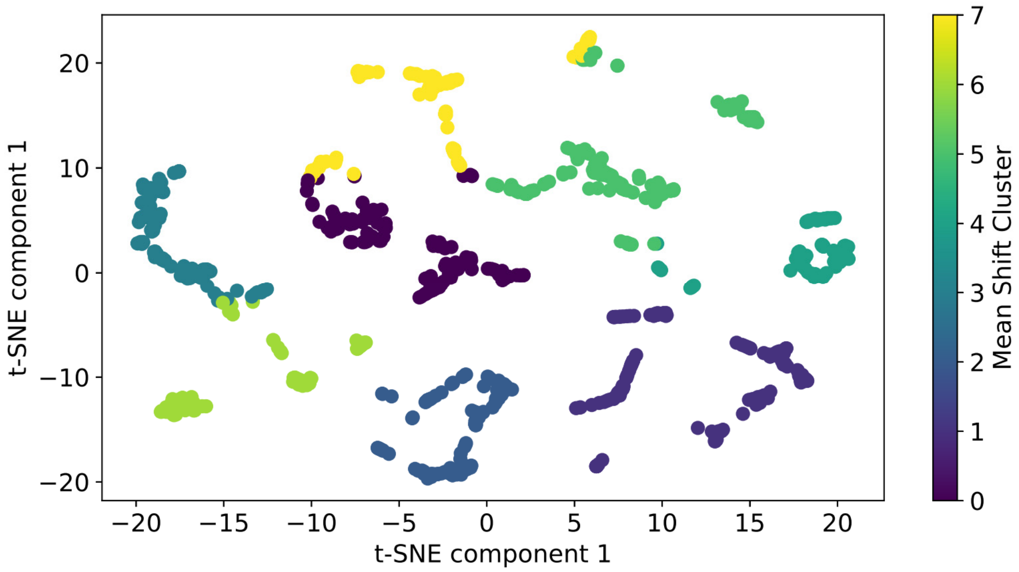

Figure 8. Visualization of the data sample after applying the Mean Shift clustering algorithm.

Table 6. Results of data sample processing.

Metrics	Value
Number of classes	8
Initial sample size	992
Sample size after class balancing	1496
Initial number of features	211
Number of features after applying the DT algorithm	18

The grid search approach was used to train the selected ML algorithms. The total dataset was divided into training and testing datasets in an 80/20 ratio. This algorithm specifies an array of variable hyperparameters for which the classification accuracy is calculated, and a set of hyperparameters is determined that provides the most satisfactory classification results. Experts specify the array of hyperparameters under consideration. Standard hyperparameter values are used for the support vector machine and restricted Boltzmann machine algorithms. Table 7 contains a description of the hyperparameters of each of the ML algorithms under consideration, an array of hyperparameter values, the selected hyperparameter value, and a brief description of each hyperparameter.

Table 7. Results of ML algorithms' hyperparameter values determining.

ML Algorithm	Hyperparameters
KNN	n_neighbors = 3
LR	C = 10
RF	n_estimators = 100, max_depth = 10, max_features = sqrt(n), min_samples_leaf = 0.02, min_samples_split = 0.005
XGBoost	n_estimators = 100, max_depth = 15, learning_rate = 0.1, base_score = 0.7
AdaBoost	n_estimators = 200, learning_rate = 0.5
CatBoost	n_estimators = 80, learning_rate = 0.1, max_depth = 10
LightBM	learning_rate = 0.1, n_estimators = 100, num_leaves = 31
SVM	C = 0.1

In Table 7, the following notations are used: n_neighbors is the number of nearest neighbors, n_estimators is the number of base classifiers, max_depth is the depth of the base classifier tree, max_features is the proportion of features of the training sample randomly selected for training one tree, n is the number of features, min_samples_leaf is the minimum proportion of data samples falling into the leaf, min_samples_split is the minimum proportion of data samples for splitting, learning_rate is the speed of learning, base_score is the base value of the probability of classifying a data row into a class for the binary case, C is the regularization parameter. Standard hyperparameters were used for the RBM algorithm.

As ML algorithms with a more complex architecture based on ANN, the convolutional neural network (CNN) and graph neural network (GNN) algorithms were considered for classifying CAs [9]. The CNN algorithm is used in most cases for recognizing image fragments; therefore, for its application, the data used were transformed into an image form, the formation scheme of which is shown in Figure 9.

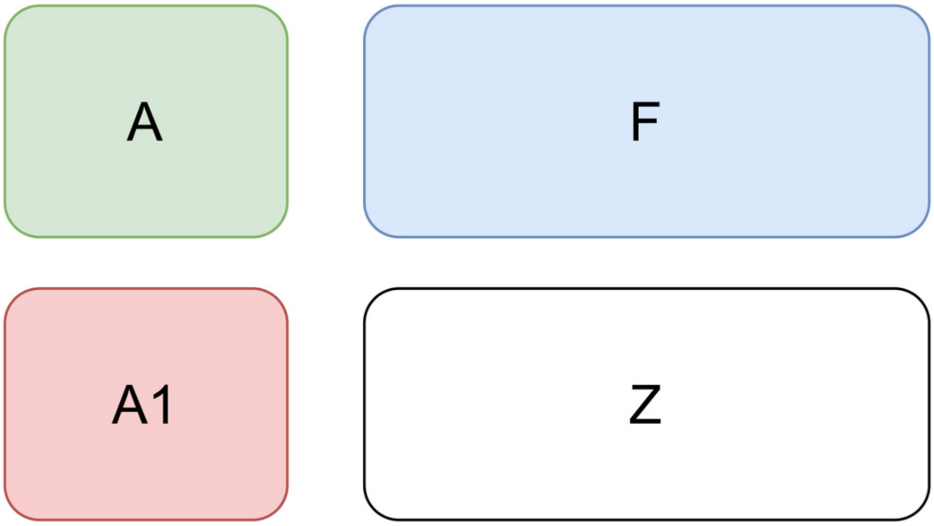

Figure 9. An example of input data for the CNN algorithm (A is the adjacency matrix of the normal EPS operating mode, A1 is the adjacency matrix of the post-accident mode, F is the feature vector, Z is an image fragment with zero values).

The structure used for the CNN algorithm is described in Table 8.

Table 8. CNN algorithm structure.

Layer	Element
Input	Image (3D tensor)
Hidden	Convolution Layer (3,3,32) Pooling layer Convolution Layer (3,3,64) Pooling layer Flatten
Output	CA class

The following parameters were used for the CNN: optimizer—Adam, learning rate—0.001, maximum epochs—30. Figure 10 shows the values of the change in errors of the CNN algorithm on the training and validation samples.

After reaching 15 training epochs, the accuracy of the CNN algorithm reaches a steady-state value, and further continuation of the training process does not lead to significant changes in accuracy.

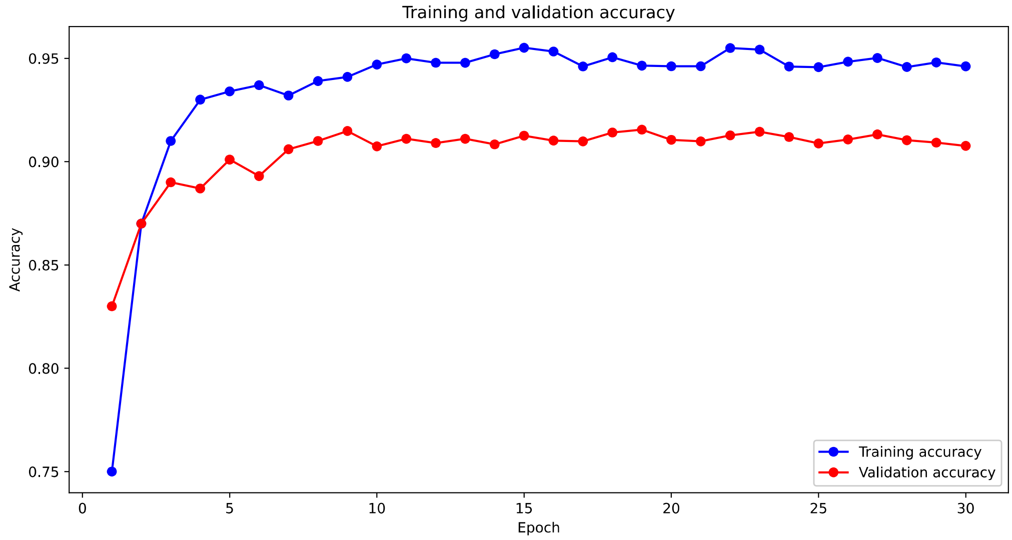

Figure 10. Modifying the accuracy of the CNN algorithm during the training process.

To select optimal CAs based on the GNN algorithm, the following parameters were used: number of layers = 5, number of units = 15, neighborhood order = 4, optimizer—RMSProp, activation function—ReLU. To incorporate information about the electrical network topology in the GNN algorithm, the adjacency matrix and electrical regime parameters are used as input data. The problem of classifying optimal CAs is considered as a graph classification problem.

Table 8 shows the classification quality metrics and the average computational delay of the CA-type classification for one mode. In Table 9, the Precision, Recall, F1 Score, and Accuracy values are given in relative units.

Table 9. Comparison of classification quality metrics of the considered ML algorithms.

Algorithm	Precision	Recall	F1_Score	Accuracy	Single Prediction Time, ms
KNN	0.835	0.835	0.835	0.835	0.071
LR	0.649	0.639	0.627	0.639	0.053
RF	0.984	0.983	0.983	0.983	0.047
XGBoost	0.960	0.950	0.950	0.954	1.150
AdaBoost	0.935	0.932	0.932	0.932	1.254
CatBoost	0.914	0.911	0.911	0.911	1.168
LightBM	0.926	0.922	0.922	0.922	0.983
SVM	0.662	0.664	0.614	0.664	0.085
RBM	0.950	0.950	0.940	0.945	0.215
CNN	0.952	0.952	0.952	0.948	0.081
GNN	0.947	0.945	0.945	0.946	0.097

The maximum classification accuracy and the shortest time to select one CA correspond to the RF algorithm, the quality metric values of which are highlighted in bold in Table 8. The lowest accuracy corresponds to the LR algorithm. The XGBoost, AdaBoost, CatBoost, and LightGBM algorithms showed similar accuracy. Figure 11 shows an example of a fragment of the RF algorithm decision tree, for which the feature numbers are indicated in the threshold value comparison expression.

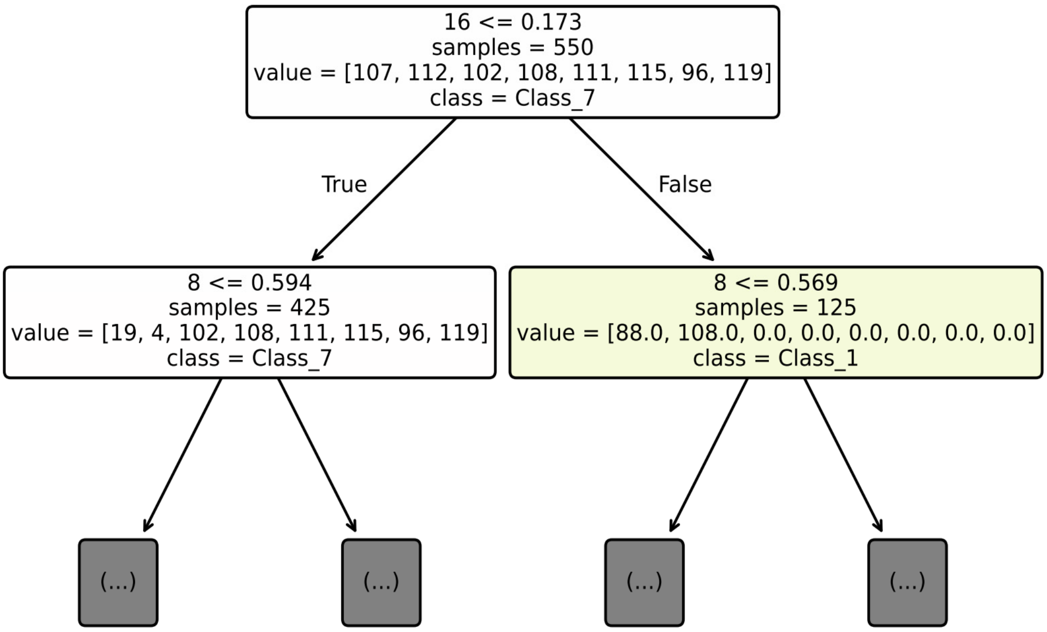

Figure 11. Example of a decision tree used in the RF algorithm.

One of the standard approaches to analyzing the quality of ML algorithm classification is to construct a confusion matrix, in which the abscissa axis indicates the classification result, the ordinate axis indicates the actual class value, and each cell of the matrix indicates the number of examples in the data sample. Constructing this matrix allows you to see the distribution of classification results [52] clearly. The main diagonal of the matrix indicates examples in which the classification result coincided with the actual CA type. The remaining elements of the matrix show erroneous classification examples. Figure 12 shows the error matrix of the random forest algorithm, for which the largest number of errors is observed for class 3.

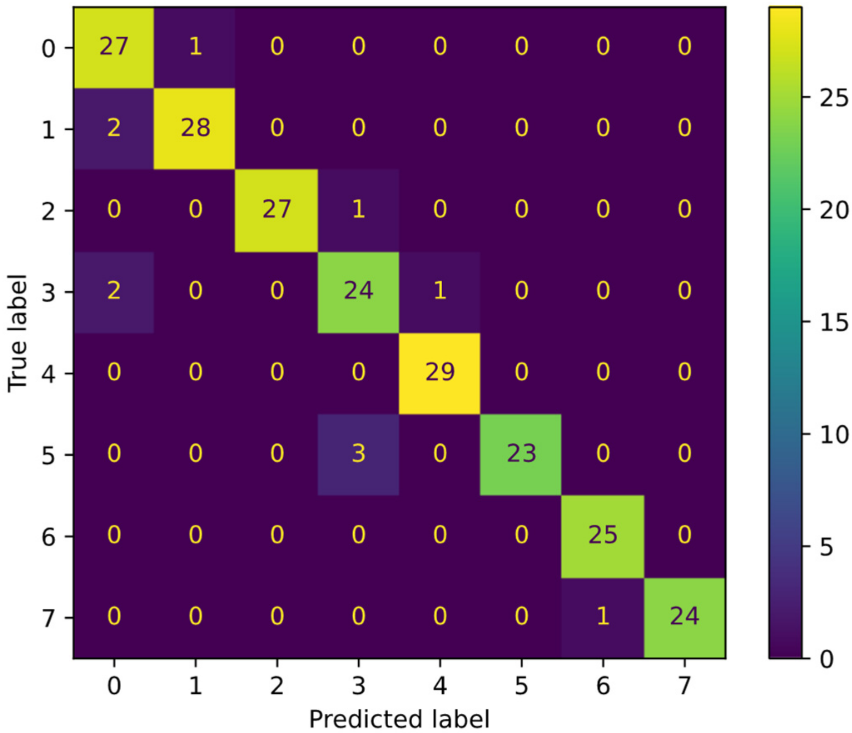

Figure 12. Confusion matrix of the RF algorithm.

Class 3 describes the SG8 GT type CA with simultaneous load shedding in node 16. The peculiarity of this CA is the minimum value of the mechanical inertia constant of SG8 compared to other SGs, which leads to an increased dynamic response of this SG to disturbances in EPS and an increase in the probability of EPS TS loss. This pattern contributes to an increase in classification errors for this CA, which is clearly shown in the error matrices.

To analyze the robustness of the technique shown in Figure 2, numerical experiments were performed with noise added to the feature signals obtained from the PMUs installed at the EPS points corresponding to the calculated informative features. Table 10 shows the results of the accuracy of CA classification by the trained RF algorithm.

Table 10. CA classification results when adding noise to informative features.

White Noise Level, dB	AC	Pink Noise Level, dB	AC	Blue Noise Level, dB	AC
0	0.983	0	0.982	0	0.984
5	0.981	5	0.981	5	0.983
10	0.980	10	0.978	10	0.982
15	0.979	15	0.976	15	0.976
20	0.973	20	0.971	20	0.972
25	0.962	25	0.961	25	0.961
30	0.954	30	0.952	30	0.956
35	0.948	35	0.949	35	0.947

Adding noise in the range from 5 to 20 dB to informative features leads to an insignificant decrease in the accuracy of CA classification. In the presence of noise interference in informative features obtained from PMU, adaptive filtering algorithms can be used [53]. The obtained CA classification delay value of 0.047 ms allows us to conclude that the RF algorithm can be used for EPS emergency control in real time.

To compare the results of the method proposed in this paper, a comparison was made with the results obtained in the study [54]. The second method used to compare the results of the proposed method is [55]. In this paper, the XGBoost algorithm was used to select optimal CAs utilizing fast valving in a steam turbine. A comparison of the methods is given in Table 11.

Table 11. CA's selection methods comparison.

EP	CA's Proposed Method	CA's [54]	CA's [55]
Line 15–16 tripping	No	No	No
Line 8–9 tripping	[SG8, Node 16]	[SG8, Node 16]	No
Line 21–22 tripping	No	No	No
Node 19 K(3) 0.2 s.	[SG4, Node 12]	[SG4, Node 12]	[SG4]
Node 22 K(2) 0.2 s.	[SG4, Node 12]	[SG4, Node 12]	[SG4]
Node 25 K(2) 0.2 s.	[SG8, Node 16]	[SG8, Node 16]	[SG8]

In Table 11, the following notations are used: K(3)—three-phase short circuit, K(2)—two-phase short circuit. In each cell with CAs, the following values are indicated in square brackets: [GT, LS].

The methods used to select CAs to ensure EPS TS, presented in this study and in [54] for the considered EPs, are entirely identical. The method presented in the study [55] allows one to determine the CA's of the GT type. The results of the method presented in the study [55] coincide with the method proposed in this study in terms of CA's of the GT type.

5. Discussion and Study Limitations

The study presents a methodology for ensuring TS in EPS with a significant share of RES, which helps to reduce the constant inertia and increase the speed of transient processes. In the context of transforming traditional EPS, the issue of maintaining TS becomes relevant [56,57]. The following are highlighted as limitations of the presented study aimed at developing a methodology for selecting optimal CAs for maintaining the TS of the protected EPS in the post-emergency operating mode:

- Traditional methods (GT and LS) of quenching excess kinetic energy arising during EP with the presence of SC are considered as CAs used to ensure the conservation of TS. In low-inertia EPS with a significant share of RES and control devices based on power electronics, it is advisable to consider CAs aimed at changing the operating mode of RES, changing the value of synthetic inertia [58], and changing the operating mode of energy storage devices. Considering a wider range of CAs allows for significantly increasing the flexibility and economic efficiency of the EPS EC process.
- The functioning of the EPS EC system based on the application of ML algorithms directly depends on the parameters of the data used for training, validation, and testing. A separate task, not considered within the framework of this article, is the development of a data synthesis methodology that ensures the representativeness, validity, and sufficiency of information required to approximate the physical patterns that arise when providing TS in the protected EPS. The solution to the data synthesis problem can be based on the use of a combination of physical measurements and synthetic data that allows considering the most severe or rare topology options and voltage levels, current loads of EPS elements, as well as active and reactive power flows along power lines or transformers [59].
- An important task, partially reflected in this study, is the development of an adaptive method for selecting informative features. The problem of selecting optimal CAs for maintaining EPS TS is characterized by a high dimensionality of the feature space describing the topology of the electrical network and the parameters of the electrical mode. To increase the speed of the training and operation of the ML algorithm, an important task is to reduce the dimensionality of the problem being solved by selecting informative features that provide the most significant contribution to the accuracy of the approximation of the law of selecting optimal CAs [29].
- When developing a methodology for selecting CAs, a separate important task is to determine the requirements for information support, including the characteristics of devices for measuring electrical mode parameters [53], the development of methods for measuring the mechanical characteristics of SG operation [60], and the determination of an acceptable speed of information exchange between the data processing center and EPS facilities where CAs are implemented.
- One of the factors, limitedly presented in this study, is the testing of the methodology for selecting optimal CAs based on physical changes characterized by the presence of noise, gaps, and outliers in the data. The use of physical data enables us to consider the practical aspects of implementing the methodology for ensuring EPS TS.
- One direction of development for the methodology, not presented in this study, is the selection of optimal CAs for predicted operating modes of the protected EPS, taking into account the topology of the electrical network and the values of active and reactive power of consumers [61].

The identified directions for future work and limitations of the study provide promising avenues for developing the proposed methodology to ensure EPS TS. In addition, one of the most important tasks that the authors set for themselves is the development of an adaptive EPS EC system that allows for the implementation of complex EPS management, taking into account the provision of all stability criteria, including new types described in the work [62].

The following are highlighted as scientific achievements of this article:

- The proposed architecture of the centralized EPS EC complex using ML algorithms is presented in Figure 1. This architecture includes the stages of generating training data, processing data to determine informative features, balancing classes, training, and testing ML algorithms. The trained ML algorithm is used for operational management of the EPS using data received from SCADA and PMU.
- A method for synthesizing synthetic data used for training and testing the ML algorithm is proposed to select optimal CAs that preserve EPS TS when EP occurs.
- An optimal ML algorithm was determined that ensures acceptable accuracy and time delay in selecting CAs to preserve EPS TS when EP occurs. RF was selected as the optimal algorithm, allowing for an accuracy of 98.3% in selecting CAs with a delay of 0.047 ms.
- An analysis of the stability of the proposed method to noise in the original data was conducted. It was determined that when adding noise of 0 to 20 dB to the original data, the accuracy of the CA's classification changes insignificantly. This proves the stability of the proposed method to noise in the original data caused by interference in the electrical mode parameter measurement system.
- The combination of data processing algorithms (SMOTE, t-SNE, Mean Shift clustering algorithm), informative feature selection (DT), and classification (RF) used in this study enables the implementation of an adaptive method for selecting optimal CAs, providing the required level of accuracy, speed, and flexibility. At the same time, the proposed method ensures high training speed, resistance to noise in the original data, and the possibility of rapid integration into the existing information infrastructure. The RF algorithm is not susceptible to overfitting due to the following features: aggregation of weak models, diversity among trees, and tree size regularization. Unlike XGBoost, where trees grow deep and risk overfitting the data, trees in RF are limited in depth or number of leaves, preventing the creation of overly detailed models.

6. Conclusions

Modern EPS are undergoing significant changes associated with a decrease in the total inertial constant, an increase in the speed, and the oscillatory component of transient processes occurring during EP occurrence. In connection with these changes, the requirements for the accuracy, adaptability, and speed of EPS control are significantly increasing. As a tool for meeting the requirements for the control of modern EPS, the use of ML algorithms is proposed. Due to the possibility of approximating hidden and implicit correlations in data, they allow synthesizing a set of decision rules that ensure the selection of optimal CAs. The use of this class of algorithms will significantly increase the speed and adaptability of optimal CAs in the conditions of modern low-inertia EPS with a significant share of RES. The article proposes the architecture of a centralized EPS EC system using ML algorithms. This complex is based on procedures for processing data from SCADA systems, PMUs, and archives of results obtained by selecting optimal CAs using deterministic algorithms [1]. By using the architecture presented in Figure 1, it is possible to organize a complete cycle of data sample preparation, its processing, training of the ML algorithm, determination of its quality metrics, and integration into the EPS operational control loop.

The paper presents a basic algorithm of a centralized EPS EC based on ML algorithms. To ensure dynamic stability, generator or load shutdowns are used as a control action choice. The functionality of the complex, based on ML algorithms, can be used as an extension of the range of capabilities of existing EPS emergency control systems. The use of CA with

ML algorithms can be beneficial in the event of accidents with cascade development, as it offers a significantly faster response compared to deterministic approaches. The article presents the analysis of studies of heuristic methods for selecting CA and estimating EPS TS based on ML algorithms. The degree of elaboration of the research topic is revealed. The advantages and disadvantages of existing heuristic methods for selecting CA are shown. The problem of selecting CA is reduced to a multiclass classification problem. A technique for selecting CA to ensure EPS TS based on ML algorithms is proposed. The technique presents the stages of data synthesis, feature selection, class balancing, as well as training and comparison of classification quality metrics on both the test and training samples. The DT algorithm with a threshold Gini coefficient of 0.03 is used to select features. The threshold value was selected through expert evaluation based on experience in researching the application of ML algorithms to the EPSEC problem. The development of a methodology for adaptively calculating the Gini coefficient threshold value is highlighted as an area for future research. The SMOTE algorithm was used to balance classes.

To determine the characteristics of the data sample, cluster analysis was used based on the Mean Shift algorithm, for the results of which the following clustering quality metrics were calculated: Silhouette coefficient, Davies-Bouldin index, Calinski-Harabasz index, Adjusted Rand index, Homogeneity score, and V-measure score. Clustering quality was assessed using several standard metrics reflecting both the internal structure of the identified clusters and their consistency with the proper class distribution. The Silhouette coefficient (0.4440), which measures the proximity of objects to their clusters compared to neighboring groups, demonstrates moderate data separation. The Davies-Bouldin index (0.7483), which measures the average ratio of intracluster dispersion to intercluster distance, also confirms the presence of a specific structure in the resulting groups. The high value of the Kalinski-Harabasz index (1187.9363) indicates a significant difference between the average distances within clusters and the overall dispersion of the sample, emphasizing the sufficient clarity of the boundaries between clusters. The Adjusted Rand Index (Adjusted Rand index = 0.5644), which measures the similarity between the actual and ideal clustering solution, approaches a value indicating a moderate degree of consistency with expectations. Finally, the Homogeneity Score (Homogeneity score = 0.5213) and V-Measure Score (V-measure score = 0.5245), which assess the homogeneity and completeness of the distribution of objects across clusters, confirm a moderate level of consistency between the resulting clustering and the predetermined data structure.

To test the CA selection methodology, the results of numerical modeling of electromechanical transient processes for the IEEE39 mathematical model were used. To reduce the total EPS inertial component, WGs were added to nodes 31, 32, 34, 35, and 38 in the EPS mathematical model used. WG output power modeling was implemented using the distributions presented in the study [43]. Eight CA classes were used to generate the synthetic dataset. The dataset size after class balancing was 1496 EPs. The number of informative features used, determined using the DT algorithm, was 18. Modeling of transient processes was performed in the Python 3 development environment in the Google Colaboratory cloud service. As a result of modeling transient processes with variation in the state of power transmission lines, loads, and generations according to a given law, a data sample was formed. To select CA, the RF algorithm was used, providing an accuracy of 98.3% with a numerical delay of 0.047 milliseconds.

Future research directions include:

- Development of a methodology for selecting CAs aimed at changing the operating mode of RES and control devices based on power electronics, considering the cost of implementing each type of control. This methodology will significantly enhance

the adaptability of EPS EC and incorporate consideration of market mechanisms for determining the composition of CAs based on the minimum control cost.
- Refinement of the synthetic data generation methodology to ensure the representativeness and validity of the EPS operating modes under consideration. Data sampling is a key task in the development of EPS control systems based on ML algorithms. The data sampling methodology proposed in this article is based on random changes in loads, generation, and the topology of the electrical network. To increase the representativeness of the data sample, a technique for targeted changes in the EPS operating mode can be used to increase the probability of EPS TS loss.
- In this study, standard ML algorithms based on ensembles of decision trees, construction of separating hyperplanes, nearest neighbors, and neural networks were applied. One of the directions for further research is the use of a multi-magnet approach and dynamic ML to increase adaptability and performance further.
- Testing the methodology on more complex EPS models: IEEE118, IEEE300, as well as on real data. A crucial task is to test the developed methodology in real-time using specialized complexes [63]. Such testing will enable us to determine the actual time costs of implementing CAs, considering the delay caused by the ML algorithm, information transmission channels, and CA implementation mechanisms on LH and GT.
- Testing of the meta, taking into account the influence of control devices based on power electronics on EPS TS [64].

Author Contributions: Conceptualization, M.S. (Mihail Senyuk) and S.B.; data curation, S.B.; formal analysis, I.Z., M.S. (Murodbek Safaraliev) and S.B. investigation, M.S. (Mihail Senyuk) and I.O.; methodology, I.Z., M.S. (Murodbek Safaraliev) and S.B.; project administration, M.S. (Murodbek Safaraliev); resources, I.Z. and S.B.; software, M.S. (Mihail Senyuk), I.O. and S.B.; supervision, I.Z.; validation, M.S. (Mihail Senyuk) and S.B.; writing—original draft, M.S. (Mihail Senyuk), S.B. and I.O.; writing—review and editing, I.Z., M.S. (Murodbek Safaraliev) and I.O. All authors have read and agreed to the published version of the manuscript.

Funding: This research received no external funding.

Data Availability Statement: The data used in our study were provided by an energy company exclusively for research purposes. According to the company's policy, they cannot be made publicly available. However, upon a justified request, the data may be provided by the authors individually for academic research.

Acknowledgments: The research funding from the Ministry of Science and Higher Education of the Russian Federation (Ural Federal University Program of Development within the Priority-2030 Program) is gratefully acknowledged.

Conflicts of Interest: The authors declare no conflict of interest.

Nomenclature

The following nomenclatures are used in this manuscript:

AdaBoost	Adaptive boosting
ANN	Artificial neural network
CA	Control actions
CatBoost	Categorical boosting
CNN	Convolutional neural network
DRL	Deep reinforcement learning
DT	Decision tree
EP	Emergency process
EPS	Electric power system
FACTS	Flexible alternating current transmission systems

GNN	Graph neural network
GT	Generator tripping
KNN	K-nearest neighbors
LightGBM	Light gradient-boosting machine
LNN	Lyapunov neural network
LR	Linear regression
LS	Load scheduling
LS-SVM	Least square support vector machine
NBC	Naive Bayes classifier NBC
NCC	Nearest centroid classifier
PCA	Principal component analysis
PMU	Phasor measurement units
RES	Renewable energy sources
RBM	Restricted Boltzmann machines
RF	Random forest
SCADA	Supervisory control and data acquisition
SG	Synchronous generator
XGBoost	eXtreme Gradient Boosting
SMOTE	Synthetic minority oversampling technique
SVM	Support vector machine
TS	Transient stability
t-SNE	t-distributed Stochastic Neighbor Embedding
WG	Wind generator

References

1. Smolovik, S.V.; Koshcheev, L.A.; Lisitsyn, A.A.; Denisenko, A.I. Special Automation for Isolated Power Systems Emergency Control. In Proceedings of the 2021 IEEE Conference of Russian Young Researchers in Electrical and Electronic Engineering (ElConRus), St. Petersburg, Moscow, Russia, 26–29 January 2021; pp. 1558–1561. [CrossRef]
2. Yang, D.; Wang, X.; Chen, W.; Yan, G.G.; Jin, Z.; Jin, E.; Zheng, T. Adaptive Frequency Droop Feedback Control-Based Power Tracking Operation of a DFIG for Temporary Frequency Regulation. *IEEE Trans. Power Syst.* **2024**, *39*, 2682–2692. [CrossRef]
3. Poulose, A.; Kim, S. Direct Transient Stability Assessment of Grid-Connected Voltage Source Converters: A Transient Energy Functions Perspective. *IEEE Access* **2024**, *12*, 133545–133556. [CrossRef]
4. Zhang, W.; Wen, Y.; Chung, C.Y. Inertia Security Evaluation and Application in Low-Inertia Power Systems. *IEEE Trans. Power Syst.* **2025**, *40*, 1725–1737. [CrossRef]
5. Nema, S.; Prakash, V.; Pandžić, H. Adaptive Synthetic Inertia Control Framework for Distributed Energy Resources in Low-Inertia Microgrid. *IEEE Access* **2022**, *10*, 54969–54979. [CrossRef]
6. Senyuk, M.D.; Klassen, V.V.; Popovtsev, V.V. Adaptive Methodology for Determining Frequency Control Law in Isolated Power Systems Based on Machine Learning Algorithms. In Proceedings of the 2024 IEEE International Multi-Conference on Engineering, Computer and Information Sciences (SIBIRCON), Novosibirsk, Russia, 30 September–2 October 2024; pp. 494–499. [CrossRef]
7. Voropai, N.I.; Efimov, D.N.; Kolosok, I.N.; Kurbatsky, V.G.; Glazunova, A.M.; Korkina, E.S.; Osak, A.B.; Tomin, N.V.; Panasetsky, D.A. Smart Technologies in Emergency Control of Russia's Unified Energy System. *IEEE Trans. Smart Grid* **2013**, *4*, 1732–1740. [CrossRef]
8. Senyuk, M.; Odinaev, I.; Pichugova, O.; Ahyoev, J. Methodology for Forming a Training Sample for Power Systems Emergency Control Algorithm Based on Machine Learning. In Proceedings of the 2023 Belarusian-Ural-Siberian Smart Energy Conference (BUSSEC), Ekaterinburg, Russia, 25–29 September 2023; pp. 54–59. [CrossRef]
9. Senyuk, M.; Beryozkina, S.; Safaraliev, M.; Pazderin, A.; Odinaev, I.; Klassen, V.; Savosina, A.; Kamalov, F. Bulk Power Systems Emergency Control Based on Machine Learning Algorithms and Phasor Measurement Units Data: A State-of-the-Art Review. *Energies* **2024**, *17*, 764. [CrossRef]
10. Chen, Q.; Zhao, Q.; Zhang, W.; Ye, H. Decentralized Robust Emergency Voltage Control of Power System with Large-Scale Wind Power Integrated via VSC-MTDC. *IEEE Trans. Ind. Appl.* **2024**, *60*, 7522–7536. [CrossRef]
11. Zhang, X.; Ono, J.P.; Song, H.; Gou, L.; Ma, K.-L.; Ren, L. SliceTeller: A Data Slice-Driven Approach for Machine Learning Model Validation. *IEEE Trans. Vis. Comput. Graph.* **2023**, *29*, 842–852. [CrossRef]

12. Kovalenko, P.Y.; Mukhin, V.I.; Senyuk, M.D.; Kornilova, D.D. Review of Methods for Power Systems State Estimation and Data Validation Based on Synchrophasor Measurements. In Proceedings of the 2020 IEEE 61st International Scientific Conference on Power and Electrical Engineering of Riga Technical University (RTUCON), Riga, Latvia, 5–7 November 2020; pp. 1–5. [CrossRef]
13. Gonzalez, V.; Torres-García, V.; Guillen, D.; Castro, L.M. Graph Theory-Based Fault Location Method for Transmission Systems with Renewable Energy Sources. *IEEE Open Access J. Power Energy* **2024**, *11*, 611–623. [CrossRef]
14. Mallinath, S.; Dutta, J.N.S.; Jadoun, V.K. Shifting of Research Trends in Fault Detection and Estimation of Location in Power System. *IEEE Access* **2025**, *13*, 70721–70740. [CrossRef]
15. Bhui, P.; Senroy, N. Real-Time Prediction and Control of Transient Stability Using Transient Energy Function. *IEEE Trans. Power Syst.* **2017**, *32*, 923–934. [CrossRef]
16. Senyuk, M.; Safaraliev, M.; Kamalov, F.; Sulieman, H. Power System Transient Stability Assessment Based on Machine Learning Algorithms and Grid Topology. *Mathematics* **2023**, *11*, 525. [CrossRef]
17. Wang, B.; Xu, Z.; Guan, X. Robust Load Frequency Control for Uncertainties Multi-Area Power Systems with Couplings of Systems Dynamics and Reconfigurable Communication Networks. *IEEE Trans. Power Syst.* **2025**, *40*, 2584–2599. [CrossRef]
18. Yan, Z.; Xu, Y. Data-Driven Load Frequency Control for Stochastic Power Systems: A Deep Reinforcement Learning Method with Continuous Action Search. *IEEE Trans. Power Syst.* **2019**, *34*, 1653–1656. [CrossRef]
19. Chen, M.; Liu, Q.; Chen, S.; Liu, Y.; Zhang, C.-H.; Liu, R. XGBoost-Based Algorithm Interpretation and Application on Post-Fault Transient Stability Status Prediction of Power System. *IEEE Access* **2019**, *7*, 13149–13158. [CrossRef]
20. Kim, J.; Lee, H.; Kim, S.; Chung, S.-H.; Park, J.H. Transient Stability Assessment Using Deep Transfer Learning. *IEEE Access* **2023**, *11*, 116622–116637. [CrossRef]
21. Chen, Q. Power System Transient Stability Assessment Model Construction Using Improved SVM. *IEEE Access* **2023**, *11*, 131866–131876. [CrossRef]
22. Zhu, Q.; Chen, J.; Zhu, L.; Shi, D.; Bai, X.; Duan, X.; Liu, Y. A Deep End-to-End Model for Transient Stability Assessment with PMU Data. *IEEE Access* **2018**, *6*, 65474–65487. [CrossRef]
23. Qiao, J.; Wang, X.; Ni, J.; Shi, M.; Ren, H.; Chen, E. Graph Neural Network Based Transient Stability Assessment Considering Topology Changes. In Proceedings of the 2021 International Conference on Power System Technology (POWERCON), Haikou, China, 8–9 December 2021; pp. 1999–2003. [CrossRef]
24. Xu, J.; Huang, J.; Wang, H. Transient Stability Assessment Considering Prediction Difficulty and Historical Training Information. *Electronics* **2025**, *14*, 57. [CrossRef]
25. Zeng, H.; Zhou, Y.; Guo, Q.; Cai, Z.; Sun, H. Distributed Deep Reinforcement Learning-based Approach for Fast Preventive Control Considering Transient Stability Constraints. *CSEE J. Power Energy Syst.* **2023**, *9*, 197–208. [CrossRef]
26. Bellizio, F.; Cremer, J.L.; Strbac, G. Transient Stable Corrective Control Using Neural Lyapunov Learning. *IEEE Trans. Power Syst.* **2023**, *38*, 3245–3253. [CrossRef]
27. Xie, Z.; Zhang, D.; Hu, W.; Han, X. Power System Transient Stability Preventive Control via Aptenodytes Forsteri Optimization with an Improved Transient Stability Assessment Model. *Energies* **2024**, *17*, 1942. [CrossRef]
28. Soni, B.P.; Saxena, A.; Gupta, V.; Surana, S.L. Transient stability-oriented assessment and application of preventive control action for power system. *J. Eng.* **2019**, *2019*, 5345–5350. [CrossRef]
29. Senyuk, M.; Odinaev, I.; Klassen, V.; Ahyoev, J. Accelerated Power System Equivalent Algorithm for Emergency Control Based on Phasor Measurement Units. In Proceedings of the 2023 Belarusian-Ural-Siberian Smart Energy Conference (BUSSEC), Ekaterinburg, Russia, 25–29 September 2023; pp. 7–12. [CrossRef]
30. Cepeda, J. Power System Dynamic Data Generation Based on Monte Carlo Simulations for Machine Learning Applications. *Eng. Proc.* **2023**, *47*, 6. [CrossRef]
31. Woźniak, A.P.; Milczarek, M.; Woźniak, J. MLOps Components, Tools, Process, and Metrics: A Systematic Literature Review. *IEEE Access* **2025**, *13*, 22166–22175. [CrossRef]
32. Yang, S.; Hao, Z.; Zhang, B.; Hojo, M. An Accurate and Fast Start-Up Scheme for Power System Real-Time Emergency Control. *IEEE Trans. Power Syst.* **2019**, *34*, 3562–3572. [CrossRef]
33. Hao, L.; Xue, Y.; Li, Z.; Wang, H.; Xu, Q. Decision Support System for Adaptive Restoration Control of Distribution System. *J. Mod. Power Syst. Clean Energy* **2022**, *10*, 1256–1273. [CrossRef]
34. Zhou, P.; Zhang, Y.; Ling, Z.; Yan, Y.; Zhao, S.; Wu, X. Online Heterogeneous Streaming Feature Selection Without Feature Type Information. *IEEE Trans. Big Data* **2024**, *10*, 470–485. [CrossRef]
35. Zhang, C.; Lu, Z.; Zhang, Y.; Dai, J. Online Streaming Feature Selection Using Bidirectional Complementarity Based on Fuzzy Gini Entropy. *IEEE Trans. Fuzzy Syst.* **2025**, *33*, 1592–1604. [CrossRef]
36. Liu, C.; Jin, S.; Wang, D.; Luo, Z.; Yu, J.; Zhou, B.; Yang, C. Constrained Oversampling: An Oversampling Approach to Reduce Noise Generation in Imbalanced Datasets with Class Overlapping. *IEEE Access* **2022**, *10*, 91452–91465. [CrossRef]
37. Aktas, H. Hyperparameter Optimization for Problem-Based Custom CNN Architectures Using a Smart Grid Search Method. *IEEE Access* **2025**, *13*, 136374–136382. [CrossRef]

38. Mishra, A.K.; Rajput, K.; Pandey, N.K.; Pathak, A. Comparative Analysis of Classification Algorithms Using Bot_IoT Dataset. In Proceedings of the 2023 International Conference on Sustainable Communication Networks and Application (ICSCNA), Theni, India, 15–17 November 2023; pp. 1775–1780. [CrossRef]
39. Kaneva, T.; Evstatiev, B.; Valova, I.; Valov, N.; Gabrovska-Evstatieva, K. Comparing Different Evaluation Metrics with the Grid Search Method for Classification of Highly Imbalanced Data. In Proceedings of the 2024 8th International Symposium on Multidisciplinary Studies and Innovative Technologies (ISMSIT), Ankara, Turkiye, 7–9 November 2024; pp. 1–5. [CrossRef]
40. Anand, S.; Mittal, S.; Tuzel, O.; Meer, P. Semi-Supervised Kernel Mean Shift Clustering. *IEEE Trans. Pattern Anal. Mach. Intell.* **2014**, *36*, 1201–1215. [CrossRef]
41. Xu, R.; Xu, J.; Wunsch, D.C. A Comparison Study of Validity Indices on Swarm-Intelligence-Based Clustering. *IEEE Trans. Syst. Man Cybern. Part B (Cybern.)* **2012**, *42*, 1243–1256. [CrossRef]
42. He, P.; Wen, B.; Wang, H. Decentralized Adaptive Under Frequency Load Shedding Scheme Based on Load Information. *IEEE Access* **2019**, *7*, 52007–52014. [CrossRef]
43. Senyuk, M.; Beryozkina, S.; Zicmane, I.; Safaraliev, M.; Klassen, V.; Kamalov, F. Bulk Low-Inertia Power Systems Adaptive Fault Type Classification Method Based on Machine Learning and Phasor Measurement Units Data. *Mathematics* **2025**, *13*, 316. [CrossRef]
44. Han, Y.; Xiu, L.; Wang, Z.; Chen, Q.; Tan, S. Artificial neural networks controlled fast valving in a power generation plant. *IEEE Trans. Neural Netw.* **1997**, *8*, 373–389. [CrossRef] [PubMed]
45. Wang, C.; Chen, S.; Mei, S.; Chen, R.; Yu, H. Optimal Scheduling for Integrated Energy System Considering Scheduling Elasticity of Electric and Thermal Loads. *IEEE Access* **2020**, *8*, 202933–202945. [CrossRef]
46. Telukunta, V.; Pradhan, J.; Agrawal, A.; Singh, M.; Srivani, S.G. Protection challenges under bulk penetration of renewable energy resources in power systems: A review. *CSEE J. Power Energy Syst.* **2017**, *3*, 365–379. [CrossRef]
47. Awad, M.; Fraihat, S. Recursive Feature Elimination with Cross-Validation with Decision Tree: Feature Selection Method for Machine Learning-Based Intrusion Detection Systems. *J. Sens. Actuator Netw.* **2023**, *12*, 67. [CrossRef]
48. Bao, Y.; Yang, S. Two Novel SMOTE Methods for Solving Imbalanced Classification Problems. *IEEE Access* **2023**, *11*, 5816–5823. [CrossRef]
49. Chatzimparmpas, A.; Martins, R.M.; Kerren, A. t-viSNE: Interactive Assessment and Interpretation of t-SNE Projections. *IEEE Trans. Vis. Comput. Graph.* **2020**, *26*, 2696–2714. [CrossRef]
50. Chu, H.-K.; Lee, T.-Y. Multiresolution Mean Shift Clustering Algorithm for Shape Interpolation. *IEEE Trans. Vis. Comput. Graph.* **2009**, *15*, 853–866. [CrossRef]
51. Bugayenko, Y.; Daniakin, K.; Farina, M.; Kholmatova, Z.; Kruglov, A.; Pedrycz, W.; Succi, G. Qualitative Clustering of Software Repositories Based on Software Metrics. *IEEE Access* **2023**, *11*, 14716–14727. [CrossRef]
52. Erbani, J.; Portier, P.-É.; Egyed-Zsigmond, E.; Nurbakova, D. Confusion Matrices: A Unified Theory. *IEEE Access* **2024**, *12*, 181372–181419. [CrossRef]
53. Senyuk, M.D.; Kovalenko, P.Y.; Mukhin, V.I.; Dmitrieva, A.A. Estimation of Acceptable ADC Sampling Rate for Synchrophasor Measurements. In Proceedings of the 2021 International Conference on Electrotechnical Complexes and Systems (ICOECS), Ufa, Russia, 16–18 November 2021; pp. 74–78. [CrossRef]
54. Glavic, M.; Ernst, D.; Ruiz-Vega, D.; Wehenkel, L.; Pavella, M. E-SIME—A method for transient stability closed-loop emergency control: Achievements and prospects. In Proceedings of the 2007 iREP Symposium—Bulk Power System Dynamics and Control—VII, Revitalizing Operational Reliability, Charleston, SC, USA, 19–24 August 2007; pp. 1–10. [CrossRef]
55. Senyuk, M.; Beryozkina, S.; Safaraliev, M.; Nadeem, M.; Odinaev, I.; Kamalov, F. Methodology for Transient Stability Enhancement of Power Systems Based on Machine Learning Algorithms and Fast Valving in a Steam Turbine. *Mathematics* **2024**, *12*, 1644. [CrossRef]
56. Alhelou, H.H.; Bahrani, B.; Ma, J.; Hill, D.J. Australia's Power System Frequency: Current Situation, Industrial Challenges, Efforts, and Future Research Directions. *IEEE Trans. Power Syst.* **2024**, *39*, 5204–5218. [CrossRef]
57. Pazderin, A.; Zicmane, I.; Senyuk, M.; Gubin, P.; Polyakov, I.; Mukhlynin, N.; Safaraliev, M.; Kamalov, F. Directions of Application of Phasor Measurement Units for Control and Monitoring of Modern Power Systems: A State-of-the-Art Review. *Energies* **2023**, *16*, 6203. [CrossRef]
58. Obaid, Z.A.; Cipcigan, L.M.; Abrahim, L.; Muhssin, M.T. Frequency control of future power systems: Reviewing and evaluating challenges and new control methods. *J. Mod. Power Syst. Clean Energy* **2019**, *7*, 9–25. [CrossRef]
59. Khalyasmaa, A.I.; Senyuk, M.D.; Eroshenko, S.A.; Plyusnina, E.I. The methodology of analysis of technical state assessment of circuit breakers. In Proceedings of the 2018 IEEE Conference of Russian Young Researchers in Electrical and Electronic Engineering (EIConRus), Moscow and St. Petersburg, Russia, 29 January–1 February 2018; pp. 667–671. [CrossRef]
60. Wu, Q.-H.; Lin, Y.; Hong, C.; Su, Y.; Wen, T.; Liu, Y. Transient Stability Analysis of Large-scale Power Systems: A Survey. *CSEE J. Power Energy Syst.* **2023**, *9*, 1284–1300. [CrossRef]

61. Cavus, M.; Allahham, A. Spatio-Temporal Attention-Based Deep Learning for Smart Grid Demand Prediction. *Electronics* **2025**, *14*, 2514. [CrossRef]
62. Hatziargyriou, N.; Milanovic, J.; Rahmann, C.; Ajjarapu, V.; Canizares, C.; Erlich, I.; Hill, D.; Hiskens, I.; Kamwa, I.; Pal, B.; et al. Definition and Classification of Power System Stability—Revisited & Extended. *IEEE Trans. Power Syst.* **2021**, *36*, 3271–3281. [CrossRef]
63. Yang, C.; Xue, Y.; Zhang, X.P.; Zhang, Y.; Chen, Y. Real-Time FPGA-RTDS Co-Simulator for Power Systems. *IEEE Access* **2018**, *6*, 44917–44926. [CrossRef]
64. Liu, C.; Li, B.; Zhang, Y.; Jiang, Q.; Liu, T. The LCC Type DC Grids Forming Method and Fault Ride-Through Strategy Based on Fault Current Limiters. *Int. J. Electr. Power Energy Syst.* **2025**, *170*, 110843. [CrossRef]